

Analytical Modeling of Bilayer Graphene Based Biosensor

Mohammad Javad Kiani^{1,2}, Ahmadi MT^{1,4*}, Elnaz Akbari³, Meisam Rahmani¹, Hediye Karimi³ and Che Harun FK¹

¹Faculty of Electrical Engineering, Universiti Teknologi Malaysia, 81310 Skudai, Johor, Malaysia

²Department of Electrical Engineering, Islamic Azad University, Yasooj Branch, Iran

³Centre for Artificial Intelligence and Robotics (CAIRO), Universiti Teknologi Malaysia, Malaysia

⁴Department of Electrical Engineering, Urima University of Technology, Iran

Abstract

Recently, great attention has been devoted to the graphene because of its unique properties, such as high charge carrier mobility even at a high charge carrier concentration at room temperature, the existence of massless Dirac fermions, Quantum Hall effect at room temperature, gas sensing at the single molecule level and gate controlled transport (electron or hole) properties. Gas concentration effect on electrical conductivity of graphene by Green function method has been modeled however sensor analytical modeling needs to be done. In this paper injected carriers by Prostate Specific Antigen (PSA) concentration are simulated and carrier controlling parameters (F, pH) are suggested. Injected carriers from PSA to the graphene surface are monitored and their effect on the capacitance is modeled. Finally comparison with experimental data which illustrates good agreement between them is considered.

Keywords: Biosensor model; PSA detection; Bilayer graphene sensor; Sensor analytical model

Introduction

Graphene is a single layer of sp²-bonded carbon atoms which arranged in a two-dimensional honeycomb lattice [1-3]. Recently numerous excellent properties of graphene such as gas sensing at the single molecule level and long spin relaxation length up to micrometer scale at room temperature direct researchers to the graphene material application [4-9]. In order to prepare single or multi-layer graphene films some methods such as thermal decomposition of commercial Silicon Carbide (SiC) substrates in vacuum, Micromechanical Cleavage (MCP) or chemical exfoliation from bulk graphite powders have been used [10-14]. Graphene has been applied in biological systems, such as detection of DNA and metal ion, protein and pathogen, design of cell/bacterial nanodevice and drug delivery carrier [15-18]. Graphene-modified electrode would facilitate electron transfer and provide a non-cytotoxic, larger surface for biomolecules immobilization because of its amazing electron transport property and high surface area [19,20]. Graphene-based sensors have the potential to detect several types of molecules and ions by itself as well as by logical, physical and chemical modification [21,22]. Cancer marker has been used as a great medical instrument in the diagnosis, monitoring and disease prediction [23,24]. General methods such as surface plasma resonance, microcantilevers and specific enzyme linked immunosorbent assay have been used to detect cancer marker [25-27]. Really PSA is a protein which produced by regular prostate cells. This enzyme plays an important role in the fertility and the dissolution of the seminal fluid coagulum [28,29]. The clinical utility of protein biomarker requires the ability to measure very low concentration proteins to diagnose health and disease [30]. The early diagnosis of many diseases such as, cancer and HIV is vital [31-33].

Since many of methods have some limitation such as ultra low detection, large detection ranges, extremely expensive and complex to realize. It is essential to provide effective approaches to design novel biosensors with nanomaterials, such as carbon nanotube and silicon nanowire with superior performance [24,31,34,35]. For example, through the binding of these biomolecules to the surface of nanostructure and based on electrical altering, carbon based nanomaterials with high sensitivity and selectivity applied to detect

small amounts of target biomolecules [22,35]. Therefore, CNTs and graphene based FETs biosensors have attracted much attention for detection of biomarker protein with high sensitivity [24,31,36]. Because of the limitations of CNTs, such as variations in electrical properties of CNT-based devices and the limited surface area of CNTs and important characteristics of graphene used in FET based biosensors is becoming more and more attractive [16-24,31,35,37]. Nevertheless, there aren't any reports on the improvement of graphene FET-based biosensors and their potential as biosensors has not been completely explored [24,37]. Consequently, it is essential to develop nanoscopic graphene based biosensors that is important criterion for biosensors because of small in size, simple in the device structure, allow label-free detection and real-time monitoring of biomarkers [24,35,37,38].

As shown in figure 1 detection method of the biosensor is demonstrated schematically. Based on the assumed detection method bilayer graphene on Polyethylene Terephthalate (PET) substrate as a sensor has been suggested. In addition low-cost, flexible and high sensitive cancer marker for real detection of PSA has been synthesized [35,39,40]. Also conductivity variation by gas molecule adsorption on graphene has been reported [41].

Model

The quantum capacitance characteristic of a BG in nanoscale is applied to evaluate the detectable PSA on graphene based biosensor. Capacitance formed between the channel and gate as most important characteristics of FET device is employed in the modeling of PSA sensor [42-45]. From classical approach, capacitance determined by physical dimensions and the dielectric constant which is between the

*Corresponding author: Ahmadi MT, Faculty of Electrical Engineering, Universiti Teknologi Malaysia, 81310 Skudai, Johor, Malaysia, E-mail: taghi@fke.utm.my

Received July 13, 2012; Accepted October 23, 2012; Published October 26, 2012

Citation: Kiani MJ, Ahmadi MT, Akbari E, Rahmani M, Karimi H, et al. (2013) Analytical Modeling of Bilayer Graphene Based Biosensor. J Biosens Bioelectron 4: 131. doi:10.4172/2155-6210.1000131

Copyright: © 2013 Kiani MJ, et al. This is an open-access article distributed under the terms of the Creative Commons Attribution License, which permits unrestricted use, distribution, and reproduction in any medium, provided the original author and source are credited.

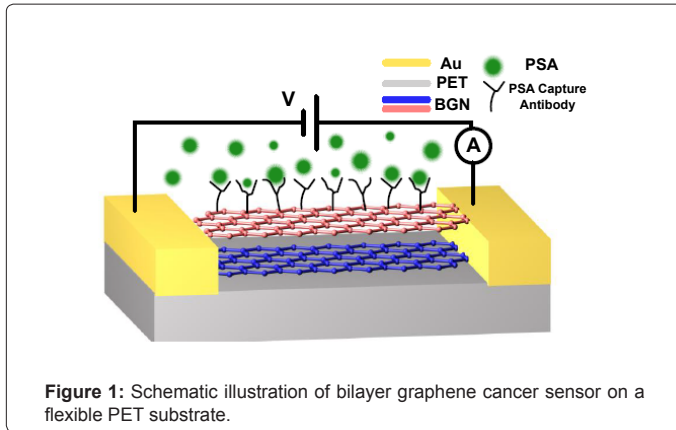


Figure 1: Schematic illustration of bilayer graphene cancer sensor on a flexible PET substrate.

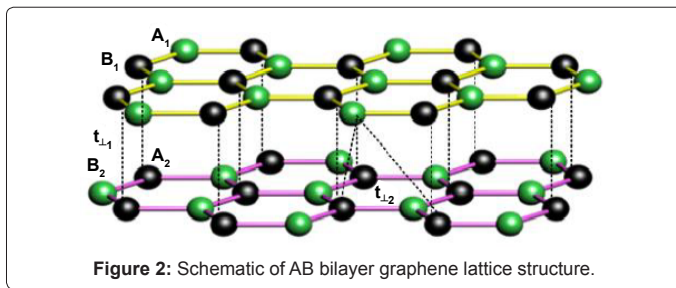


Figure 2: Schematic of AB bilayer graphene lattice structure.

electrodes [46,47]. The conductance of graphene as a function of carrier density and mobility experimentally have been reported which means changes in density and/or charge carriers by adsorption of molecules or ions in graphene will affect the conductance [35]. In the proposed model PSA adsorption as a source of attached carriers is assumed. As shown in figure 1 two Au electrodes of the sensor can be suggested as the source and drain and Dc voltage (V) is applied to them. Also carrier concentration can be modeled by the carrier concentration of BG (n) plus the carrier concentration (n') injected from PSA.

$$\partial Q = e\partial(n + n') \quad (1)$$

Where ∂Q is the change in charge per unit length, n is the intrinsic carrier concentration and n' is the inject carriers by PSA.

Bilayer graphene as a channel material has been explored [44]. Two different stacking configurations (AA and AB) are obtained for (BGs) with armchair edge. The AA-stacked which is metallic and the AB-stacked whereas having a band gap of 0.02 eV, is a semiconductor that is in our focus. In AB structure, atoms on top layer of BG called (A2, B2) and bottom layer are (A1, B1) with hexagonal carbon lattice in figure 2. Near to the K point the electronic dispersion of BG can be written as [44,45]:

$$E(k) \approx (V/2) - \alpha k^2 + \beta k^2 \quad (2)$$

Where $\beta = v_F^4 / V_{t1}^2$, $\alpha = (V / t_1^2) v_F^2$, V is bias voltage and Fermi velocity is $v_F = 3ta_{c-c} / 2$. In-plan hopping t is about equivalent to 3.1 (eV), t_{\perp} is an interlayer hopping (the experimental value for bulk graphite is approximately equal to 0.39 eV). Density of state (DOS) as basic parameters on BG shows available energy states. It is notable that electrical property of materials from metal to semiconducting is changing by the gradient of DOS near the Dirac point.

$$D(E) = \frac{1}{2\pi(4\beta k^3 - 2\alpha k)} \quad (3)$$

Carrier concentration in a band can be achieved by integrating the distribution function over energy band.

$$n = \int \left(2\pi(4\beta \left[\frac{\alpha \pm \sqrt{\alpha^2 - 4(E-V/2)\beta}}{2\beta} \right]^{\frac{3}{2}} - 2\alpha \left[\frac{\alpha \pm \sqrt{\alpha^2 - 4(E-V/2)\beta}}{2\beta} \right]^{\frac{1}{2}} \times (1+\eta) \right)^{-1} dE \quad (4)$$

Where, $\eta = e^{\frac{E-E_F}{k_B T}}$ is normalized Fermi energy. In order to model the effect of PSA adsorption by graphene we have monitored capacitance variation as:

$$C_q = e^2 \frac{\partial n}{\partial E} + e^2 \frac{\partial n'}{\partial E} \quad (5)$$

It has been demonstrated that the conductance of biosensor depends on the concentration of PSA and different local pH values. Carrier concentration as a function of PSA concentration and different local pH values is considered, which are presented in the form of PSA and PH factors (f,p). The carriers injected from the PSA and localized pH value into the bilayer graphene is added to the conventional carrier concentration as:

$$n' = fF_{PSA} + pP_H \quad (6)$$

So the capacitance based on the proposed model of BG carriers and adsorbing carriers (PSA) by the surface of the biosensor is modified as:

$$C_q = e^2 \left(2\pi \left(4\beta \left[\frac{\alpha \pm \sqrt{\alpha^2 - 4(E-V/2)\beta}}{2\beta} \right]^{\frac{3}{2}} - 2\alpha \left[\frac{\alpha \pm \sqrt{\alpha^2 - 4(E-V/2)\beta}}{2\beta} \right]^{\frac{1}{2}} \times (1+\eta) \right)^{-1} + e^2 f \frac{\partial F}{\partial t} \frac{\partial t}{\partial E} + e^2 p \frac{\partial P_H}{\partial t} \frac{\partial t}{\partial E} \right) \quad (7)$$

Where ∂F is the PSA concentration, variation and ∂P_H is different in local pH values, therefore the current voltage characteristic can be modified by proposing capacitance model as:

$$I = \left(e^2 \left(2\pi \left(4\beta \left[\frac{\alpha \pm \sqrt{\alpha^2 - 4(E-V/2)\beta}}{2\beta} \right]^{\frac{3}{2}} - 2\alpha \left[\frac{\alpha \pm \sqrt{\alpha^2 - 4(E-V/2)\beta}}{2\beta} \right]^{\frac{1}{2}} \times (1+\eta) \right)^{-1} + e^2 f \frac{\partial F}{\partial t} \frac{\partial t}{\partial E} + e^2 p \frac{\partial P_H}{\partial t} \right) \times V_{ds} \mu_e E \right) \quad (8)$$

As shown in figure 3 current-voltage characteristic of graphene based PSA biosensor by the quantum capacitance effect is plotted. Based on the experimental data it is explored that Sensor I-V characteristic can be controlled by PSA concentration (as an antibodies parameter), therefore the concentration coefficient by iteration method is estimated as:

$$f = f_1 \ln(F) + f_2 \quad (9)$$

Where $f_1 = 1.84 \cdot 10^{-2}$ and $f_2 = 0.3991$

As shown in figures 3 and 4, after incubating bio sensor in different concentrations of PSA and labeled by HRP the normalized conductance of graphene not only raises with the increasing of PSA concentration but also conductance of the bilayer graphene changes with the different local pH values. Thus the pH effect on the carrier concentration in the same manner with PSA concentration by iteration method is modeled as:

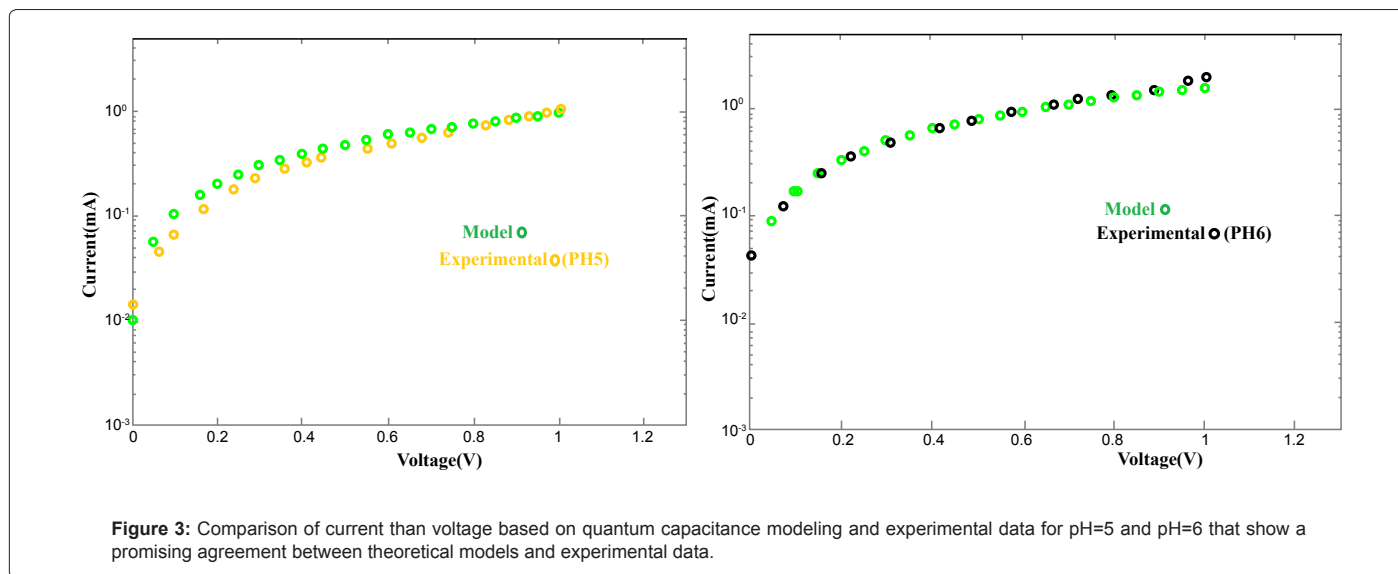


Figure 3: Comparison of current than voltage based on quantum capacitance modeling and experimental data for pH=5 and pH=6 that show a promising agreement between theoretical models and experimental data.

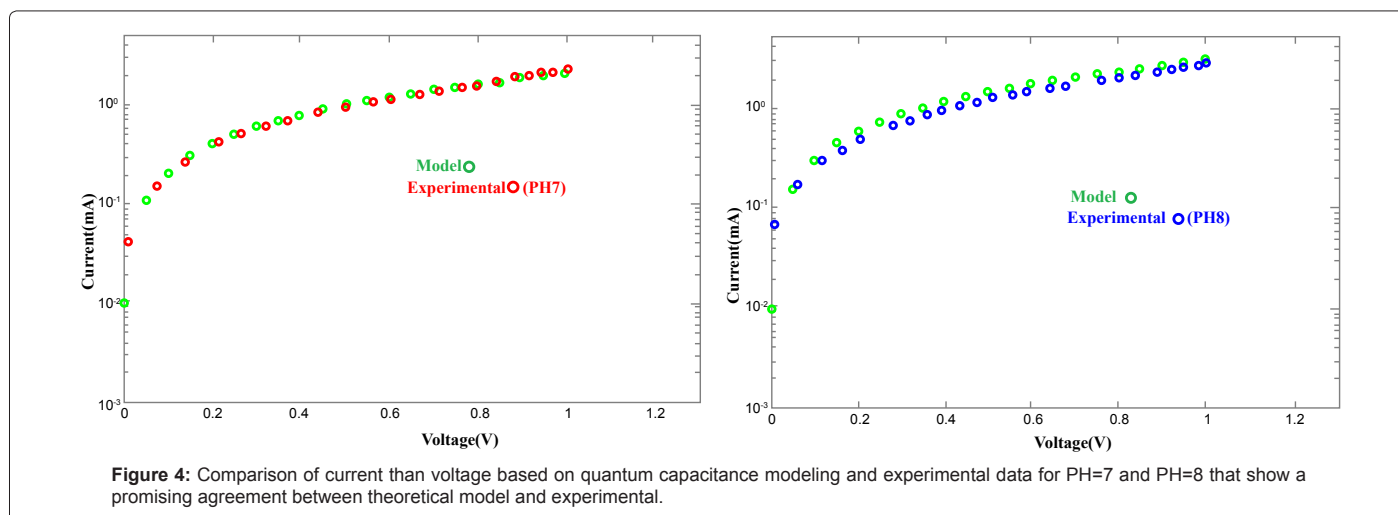


Figure 4: Comparison of current than voltage based on quantum capacitance modeling and experimental data for PH=7 and PH=8 that show a promising agreement between theoretical model and experimental.

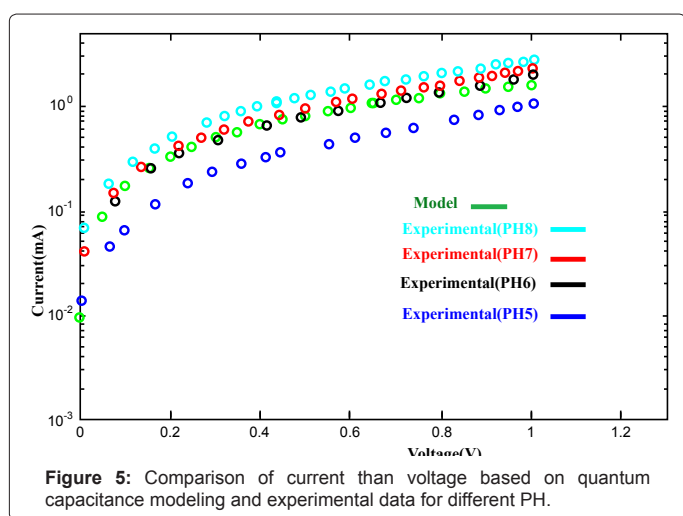


Figure 5: Comparison of current than voltage based on quantum capacitance modeling and experimental data for different PH.

$$p = p_1 P_H^2 - p_2 P_H + p_3 \quad (10)$$

Where $p_1=170.31$, $p_2=15.063$ and $p_3=5.3251$. Also the suggested PSA detection modelling can be employed for almost any target antigen with a known antibody.

$$I = \left[e^2 \left(2\pi \left[4\beta \left[\frac{\alpha \pm \sqrt{\alpha^2 - 4(E-V/2)\beta}}{2\beta} \right]^3 - 2\alpha \left[\frac{\alpha \pm \sqrt{\alpha^2 - 4(E-V/2)\beta}}{2\beta} \right]^2 \right) \times (1+\eta) \right)^{-1} + \right] \times V_{as} \mu_e E \quad (11)$$

$$e^2 (1.84 \times 10^{-3} \ln(F) + 0.3991) \frac{\partial F}{\partial t} \frac{\partial t}{\partial E} + e^2 (170.31 P_H^2 - 15.063 P_H + 5.3251) P_H$$

As shown in figure 5 based on the presented model it is notable that by raising the concentration (as an example for pH value is 6) model is closer to the experimental data (black line). In the same manner we can compare other experimental data's as well.

Current-voltage characteristic altering by carrier concentration and local pH values, also based on the supposed model sensor I-V characteristic which is controlled by PSA concentration parameter and PH parameter.

Conclusion

Graphene based material because of its amazing electron transport

property and high surface area has been employed in biological applications. Green function method in the gas sensor modeling has been used although pH physical based sensor modeling needs to be explored. In this research current voltage characteristic of a BG in terms of capacitance model is applied to evaluate the detectable PSA on the graphene based biosensors. PSA adsorption and local pH value effects on the carrier concentration are monitored and injected carriers as a function of control parameters (f, p) are presented. Finally, good agreement between proposed model and experimental data is reported. We have concluded that sensor characteristics altered by PSA concentration and local pH values, by means of which the proposed model sensor can be controlled.

Acknowledgments

Authors would like to acknowledge the financial support from Research University grant of the Ministry of Higher Education (MOHE), Malaysia under Projects Q.J130000.7123.02H24. Also thanks to the Research Management Center (RMC) of University Teknologi Malaysia (UTM) for providing excellent research environment in which to complete this work.

References

1. Amini M, Jafari SA, Shahbazi F (2009) Anderson transition in disordered graphene. *Europhys Lett* 87.
2. Ataca C, Sahin H, Akturk E, Ciraci S (2011) Mechanical and Electronic Properties of MoS₂ Nanoribbons and Their Defects. *J Phys Chem C Nanomater Interfaces*. 115: 3934-3941.
3. Cuansing E, Wang JS (2009) Quantum transport in honeycomb lattice ribbons with armchair and zigzag edges coupled to semi-infinite linear chain leads. *Eur Phys J B* 69: 505-513.
4. Gibertini M, Singha A, Pellegrini V, Polini M (2009) Engineering artificial graphene in a two-dimensional electron gas. *Physical Review B* 79.
5. Zarbo LP, Nikolic BK (2007) Spatial distribution of local currents of massless Dirac fermions in quantum transport through graphene nanoribbons. *Europhys Lett* 80.
6. Burgess CP, Dolan BP (2007) Quantum Hall effect in graphene: Emergent modular symmetry and the semicircle law. *Phys Rev B* 76.
7. Ni GX, Zheng Y, Bae S, YawTan C, Kahya O, et al. (2010) P Graphene-based memory cell for non-volatile memory, has graphene layer having controllable resistance states representing data values of the cell and ferroelectric layer controlling the resistance states. *Univ Singapore Nat*.
8. Zou Y, Li F, Zhu ZH, Zhao MW, Xu XG, et al. (2011) An ab initio study on gas sensing properties of graphene and Si-doped graphene. *Eur Phys J B* 81: 475-479.
9. Chai Y, Gong J, Zhang K, Chan PC, Yuen MM (2007) Flexible transfer of aligned carbon nanotube films for integration at lower temperature. *Nanotechnology* 18.
10. Kulkarni AJ, Zhou M, Ke FJ (2005) Orientation and size dependence of the elastic properties of zinc oxide nanobelts. *Nanotechnology* 16: 2749-2756.
11. Ang PK, Wang S, Bao Q, Thong JT, Loh KP (2009) High-Throughput Synthesis of Graphene by Intercalation - Exfoliation of Graphite Oxide and Study of Ionic Screening in Graphene Transistor. *Acs Nano* 3: 3587-3594.
12. Berger C, Song Z, Li T, Li X, Ogbazghi AY, et al. (2004) Ultrathin epitaxial graphite: 2D electron gas properties and a route toward graphene-based nanoelectronics. *J Phys Chem B* 108: 19912-19916.
13. Sarkar S, Das PK, Bysakh S (2011) Effect of heat treatment on morphology and thermal decomposition kinetics of multiwalled carbon nanotubes. *Mater Chem Phys* 125: 161-167.
14. JK, Aryasomayajula L, Whitchurch A, Varadan VK (2008) Carbon nanotube strain sensors for wearable patient monitoring applications. *Nanosensors and Microsensors for Bio-Systems 2008* 6931: J9310-J9310.
15. Qiu Y, Qu X, Dong J, Ai S, Han R (2011) Electrochemical detection of DNA damage induced by acrylamide and its metabolite at the graphene-ionic liquid-Nafion modified pyrolytic graphite electrode. *J Hazard Mater* 190: 480-485.
16. Bertini I, Lee YM, Luchinat C, Piccioli M, Poggi L (2001) Locating the metal ion in calcium-binding proteins by using cerium(III) as a probe. *Chembiochem* 2: 550-558.
17. Ohno Y, Maehashi K, Yamashiro Y, Matsumoto K (2009) Electrolyte-Gated Graphene Field-Effect Transistors for Detecting pH Protein Adsorption. *Nano Letters* 9: 3318-3322.
18. Lin L, Liu Y, Tang L, Li J (2011) Electrochemical DNA sensor by the assembly of graphene and DNA-conjugated gold nanoparticles with silver enhancement strategy. *Analyst* 136: 4732-4737.
19. Liao KH, Lin YS, Macosko CW, Haynes CL (2011) Cytotoxicity of Graphene Oxide and Graphene in Human Erythrocytes and Skin Fibroblasts. *Acs Appl Mater Interfaces* 3: 2607-2615.
20. Baby TT, Aravind SS, Arockiadoss T, Rakhi RB, Ramaprabhu S (2010) Metal decorated graphene nanosheets as immobilization matrix for amperometric glucose biosensor. *Sens Actuators B Chem* 145: 71-77.
21. Xie Y, Chen A, Du D, Lin Y (2011) Graphene-based immunosensor for electrochemical quantification of phosphorylated p53 (S15). *Anal Chim Acta* 699: 44-48.
22. Myung S, Solanki A, Kim C, Park J, Kim KS, et al. (2011) Graphene-Encapsulated Nanoparticle-Based Biosensor for the Selective Detection of Cancer Biomarkers. *Advanced Materials* 23: 2221-2225.
23. Alwarappan S, Erdem A, Liu C, Li C (2009) Probing the Electrochemical Properties of Graphene Nanosheets for Biosensing Applications. *J Phys Chem C* 113: 8853-8857.
24. Alwarappan S, Boyapalle S, Kumar A, Li C, Mohapatra S (2012) Comparative Study of Single-, Few-, and Multilayered Graphene toward Enzyme Conjugation and Electrochemical Response. *J Phys Chem C Nanomater Interfaces* 116: 6556-6559.
25. Siva P, Krithika N, Zhongcheng G, David M, Long Q (2010) Biological cell controllable patch-clamp microchip. *Applied Physics Letter* 97: 263702-263702.
26. Alwarappanab S, Singh SR, Pillaid SK, Kumar A, Mohapatra S (2012) Direct Electrochemistry of Glucose Oxidase at a Gold Electrode Modified with Graphene Nanosheets. *Anal Lett* 45: 746-753.
27. Nagaraj VJ, Aithal S, Eaton S, Bothara M, Wiktor P (2010) Nano Monitor: a miniature electronic biosensor for glycan biomarker detection. *Nanomedicine* 5: 369-378.
28. Hara M, Koyanagi Y, Inorre T, Fukuyama T (1971) Some physicochemical characteristics of gamma-seminoprotein, an antigenic component specific for human seminal plasma. *Nihon Hoigaku Zasshi* 25:322-324.
29. Li TS, Beling CG (1973) Isolation and characterization of two specific antigens of human seminal plasma. *Fertil Steril* 24:134-144.
30. Bin X, Sargent EH, Kelley SO (2010) Nanostructuring of Sensors Determines the Efficiency of Biomolecular Capture. *Analytical Chemistry* 82: 5928-5931.
31. Du D, Zou Z, Shin Y, Wang J, Wu H, et al. (2010) Sensitive Immunosensor for Cancer Biomarker Based on Dual Signal Amplification Strategy of Graphene Sheets and Multienzyme Functionalized Carbon Nanospheres. *Analytical Chemistry* 82: 2989-2995.
32. Batman G, Oliver AW, Zehbe I, Richard C, Hampson L, et al. (2011) Lopinavir up-regulates expression of the antiviral protein ribonuclease L in human papillomavirus-positive cervical carcinoma cells. *Antivir Ther* 16: 515-525.
33. Javanmard M, Talasaz AH, Nemat-Gorgani M, Pease F, Ronaghi M, et al. (2009) Electrical detection of protein biomarkers using bioactivated microfluidic channels. *Lab Chip* 9: 1429-1434.
34. Abdelwahab AA, Koh WC, Noh HB, Shim YB, et al. (2010) A selective nitric oxide nanocomposite biosensor based on direct electron transfer of microperoxidase: removal of interferences by co-immobilized enzymes. *Biosens Bioelectron* 26: 1080-1086.
35. Zhang B, Cui T (2011) An ultrasensitive and low-cost graphene sensor based on layer-by-layer nano self-assembly. *Appl Phys Lett* 98.
36. Alwarappan S, Liu G, Li CZ (2010) Simultaneous detection of dopamine, ascorbic acid, and uric acid at electrochemically pretreated carbon nanotube biosensors. *Nanomedicine* 6: e52-e57.
37. Alwarappan S, Prabhulkar S, Durygin A, Chen-Zhong L (2009) The Effect of Electrochemical Pretreatment on the Sensing Performance of Single Walled Carbon Nanotubes. *J Nanosci Nanotechnol* 9: 2991-2996.

38. Chen F, Qing Q, Xia J, Tao N (2010) Graphene Field-Effect Transistors: Electrochemical Gating, Interfacial Capacitance, and Biosensing Applications. *Chem Asian J* 5: 2144-2153.
39. Truong PL, Kim BW, Sim SJ (2012) Rational aspect ratio and suitable antibody coverage of gold nanorod for ultra-sensitive detection of a cancer biomarker. *Lab Chip* 12: 1102-1109.
40. Lee SM, Hwang KS, Yoon HJ, Yoon DS, Kim SK, et al. (2009) Sensitivity enhancement of a dynamic mode microcantilever by stress inducer and mass inducer to detect PSA at low picogram levels. *Lab Chip* 9: 2683-2690.
41. Mousavi H (2011) Graphene as Gas Sensors. *Commun Theor Phys* 56: 373-376.
42. Stoller MD, Magnuson CW, Zhu Y, Murali S, Suk JW, et al. (2011) Interfacial capacitance of single layer graphene. *Energy Environ Sci* 4: 4685-4689.
43. Amin NA, Ahmadi MT, Johari Z, Mousavi SM, Ismail R, et al. (2011) Effective mobility model of graphene nanoribbon in parabolic band energy. *Modern Phys Lett B* 25: 739-745.
44. Karamdel J, Ahmadi MT, Damghanian M, Majilis BY, Dee CY, et al. (2009) Analysis and simulation of carriers statistic for semiconducting single wall carbon nanotube. *Materials Research Innovations* 13: 211-213.
45. Appenzeller J, Sui Y, Chen ZH (2009) Graphene nanostructures for device applications. 2009 Symposium on Vlsi Technology, Digest of Technical Papers: 124-126.
46. Mukherjee S, Manninen M, Singha PD (2011) Quantum capacitance: A microscopic derivation. *Physica E Low Dimens Syst Nanostruct* 44: 62-66.
47. Krowne CM (2010) Intrinsic quantum conductances and capacitances of nanowires and nanocables. *Phys Lett A* 374: 614-619.